Preprints of the 19th World Congress
The International Federation of Automatic Control
Cape Town, South Africa. August 24-29, 2014

Robust Real-time Optimal Autonomous Highway Driving Control System: Development and Implementation

Seung-Hi Lee * **Youngseop Son** ** **Chung Choo Chung** ***

* *Div. of Electrical and Computer Engineering, Hanyang University, Korea (e-mail: shlee@ieee.org).*
** *Global R&D Center, MANDO Corporation, Korea (email: ysson@mando.com).*
*** *Div. of Electrical and Computer Engineering, Hanyang University, Korea (e-mail: cchung@hanyang.ac.kr).*

Abstract: This paper develops a systems approach for robust real-time optimal autonomous driving control system development. An autonomous vehicle control system framework is proposed to dissect an automotive system into some sub-systems in which physical systems and control softwares are communicating. To attain robustness, a robust on-road vehicle localization scheme is proposed applying multi sensor-data fusion with the results of multirate decentralized state estimation and the clothoidal road model constraint. Control block and control block topology are proposed to utilize block-wise perception of environment and vehicle localization and to produce a trajectory command via a virtual lane curve for longitudinal/lateral vehicle control. To attain real-time control optimality, we apply the multilevel approximate predictive control developed by the authors. Performance of the proposed autonomous driving control system is demonstrated through some track test results.

1. INTRODUCTION

Autonomous driving vehicles are said to be the future of automotive vehicles that provide safety, comfortability, convenience for drivers. Autonomous vehicles accordingly become a very important research topic in the automotive industry.

Autonomous driving control requires much more advanced control technologies over adaptive cruise control and lane keeping control which assist the driver's driving action by getting the information of road environment and vehicle's states. Autonomous driving control thus requires lateral as well as longitudinal motion control. Many articles considered lateral control design such as automated lane change steering control (see e.g. Falcone et al. (2007); Guldner et al. (1999); Hatipoglu et al. (2003)). It is however hard to find control designs that consider both lateral and longitudinal motion control, whilst there has been so much work on lane keeping/changing control design. It is our experience that adjusting the longitudinal velocity according to the vehicle's yaw rate and/or speed tends to provide more efficient driving (e.g. lane changing). Almost no article considers longitudinal velocity control in the lane changing control. Longitudinal vehicle control was mostly for intelligent vehicle highway system (IVHS) (see e.g., Hedrick et al. (1991); Pham et al. (1994)). In Pham et al. (1994), combined lateral and longitudinal control was presented for IVHS. In Rajamani et al. (2000), integrated longitudinal and lateral control was presented. Cruise control (see e.g., Ioannou et al. (1993); Möbus et al. (2003)) is also an interesting vehicle longitudinal control problem.

Multirate sensing is inherent in autonomous vehicles and it causes control system design to become challenging. Recent trends in the lane keeping/changing system research are using vision systems to obtain optical lane recognition (Dickmanns (2002)) which are slow. Whilst, other measurements such as the yaw rate and the longitudinal velocity are available at a fast rate through the vehicle's electronic control unit (ECU). It is well known that the performance of a digital control system is limited by the applied sampling rate. Nonetheless, the approach of conventional lateral control is to generate a control command at the same slow rate of the vision processing. The problem of a slow update rate as well as the time delay of vision processing systems causes inaccurate control and undesirable lateral behavior such as oscillatory responses due to the loss of damping.

Applying predictive control is prospective for real-time optimality in the presence of various constraints (e.g. steering angle limit and its rate limit, yaw rate limit, etc.), provided it can be solved in real-time. No other control methods can consider such various constraints. In this regard, the authors proposed an innovative approximate explicit model predictive control (MPC) strategy applying multilevel approximation scheme (Lee and Chung (2013)). The scheme achieved a significant improvement of

[1] This work was supported by National Research Foundation of Korea Grant funded by the Korean Government (2012R1A1A2044762). This work was also supported by the Industrial Source Technology Development Program(10044620, Automatic lane change system for novice drivers) funded by the Ministry of Trade, Industry and Energy(MOTIE, Korea).

computation time and approximation quality over other approximate predictive control methods. Applications of MPC to vehicle motion control are very promising and numerous successful results have been reported so far (see e.g. Falcone et al. (2007); Li et al. (2010)).

The paper develops an autonomous driving control system in a systems approach, with robust lane curve estimation and control performance optimality. We will propose a new paradigm for autonomous driving control system design, and develop a set of sub-system modelings. We are to introduce innovative methods for block-wise perception of environment around the vehicle and for determining admissible maneuvering to design trajectory commands. Robust real-time optimality is to be attained by developing a robust road lane estimation scheme and by applying predictive control scheme developed by the authors Lee and Chung (2013). We are also to demonstrate the performance of the proposed autonomous driving control system through in-vehicle tests and some track test results.

NOMENCLATURE

$\{XYZ\}$ inertial coordinate frame
$\{xyz\}$ local coordinate frame
'O' the center of turn (CT)
x a front fixed longitudinal position in $\{xyz\}$
y lateral position of the origin of $\{xyz\}$ to CT
y_{des} lateral position of the lane center to CT
$\dot{x} = V_x$ longitudinal velocity at the center of gravity (CG)
$\dot{y} = V_y$ lateral velocity at CG of vehicle
ψ yaw, heading, angle of vehicle in $\{XYZ\}$
ψ_{des} yaw, heading, angle of the lane center in $\{XYZ\}$
β vehicle side slip angle at CG
α_f (α_r) front (rear) tire slip angle
$\dot{\psi}$ yaw rate of vehicle
δ_f (δ_r) front (rear) steering angle
C_α ($C_{\alpha f}$, $C_{\alpha r}$) cornering stiffness of (front, rear) tire
F_y (F_{yf}, F_{yr}) lateral force on (front, rear) tire
θ_V tire velocity angle in $\{xyz\}$
ϕ road bank angle
μ Tire-road friction coefficient
R turn radius of vehicle or radius of road
L look-ahead distance
$e_y = y - y_{des}$ lateral position error in $\{xyz\}$
$e_\psi = \psi_{\text{des}} - \psi$ heading angle error in $\{xyz\}$
N steering ratio
m total mass of vehicle
I_z yaw moment of inertia of vehicle
l_f (l_r) longitudinal distance: CG to front (rear) tire
$l_{fr} = l_f + l_r$ wheelbase

PARAMETER DEFINITIONS

$$a_{22} = -\frac{2C_{\alpha f} + 2C_{\alpha r}}{mV_x},\ a_{23} = -a_{22}V_x,$$
$$a_{24} = -1 - \frac{2C_{\alpha f}l_f - 2C_{\alpha r}l_r}{mV_x^2},\ a'_{24} = (a_{24} - 1)V_x,$$
$$a_{42} = -\frac{2C_{\alpha f}l_f - 2C_{\alpha r}l_r}{I_z},\ a'_{42} = \frac{a_{42}}{V_x},\ a_{43} = -a_{42},$$
$$a_{44} = -\frac{2C_{\alpha f}l_f^2 + 2C_{\alpha r}l_r^2}{I_z V_x},$$
$$b_{21} = \frac{2C_{\alpha f}}{mV_x},\ b'_{21} = b_{21}V_x,\ b_{41} = \frac{2C_{\alpha f}l_f}{I_z}.$$

2. PROBLEM DESCRIPTION

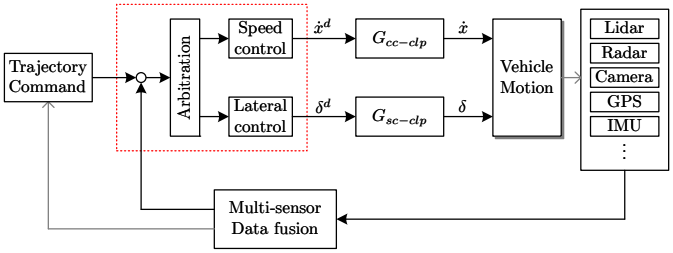

Fig. 1. Autonomous Driving Control Framework

We are interested in developing a new paradigm for autonomous driving control design and implemenation as shown in Fig. 1. The framework dissects a complex automotive system into some accessible cyber-physical subsystems (consisting of physical systems and control softwares, with communications between them). The proposed paradigm has a significant advantage of allowing cyber-physical systems approach: one can independently determine each sub-system or control software while just considering possible high-level communication between them. One can thus easily apply well developed variety of control and estimation theories. Seamless integration into vehicles is quite natural because the communication is already well defined.

We are thus interested in developing some essential techniques to realize autonomous driving in the proposed autonomous driving framework. Specifically, we are interested in developing cyber-physical sub-system modelings, developing vehicle localization and environment perception, designing the 'trajectory command' and the 'arbitration', the 'speed control', and the 'lateral control'. For reliable vehicle localization and environment perception, we are interested in developing a multirate decentralized state estimator based multi sensor-data fusion. In regard to a trajectory command, we are interested in developing an innovative method that can efficiently describe the condition of vehicle's environment in pursue of safest autonomous maneuvering.

3. SUB-SYSTEM MODELING

In order to deal with the autonomous driving control framework shown in Fig. 1, let us develop a unique set of cyber-physical sub-system modelings. The figure dissects the automotive system into some sub-systems to be modeled. By the cyber-physical sub-system modeling we mean that we model the sub-systems that are either physical system or cyber-physical: real physical system motion, (control) softwares, or approximations of concepts/phenomena. We are to develop a high-level vehicle motion model transfer function from $\begin{bmatrix}\dot{x}^d & \delta^d\end{bmatrix}^T$, the desired longitudinal velocity and steering angle, to the vehicle pose in terms of road lane curve tracking error at a look-ahead distance error. We also develop the cruise control closed-loop G_{cc-clp} to describe the high-level longitudinal motion and the steering control closed-loop G_{sc-clp}. By combining them we are to build a high-level vehicle motion model.

3.1 Lateral Motion Model

In highway driving, it is quite practical to assume steady state tire deformation, small tire slip angle, and (almost) constant μF_z. In this case, the lateral tire force modeling becomes simple: the tire lateral force F_y can be approximately represented by tire slip angle α and a constant cornering stiffness $C_{\alpha f}$ such that $F_y = C_{\alpha f}\alpha$. For large tire slip angles, we need to introduce more sophisticated nonlinear tire model such as Pacejka's magic formula curve (Pacejka et al. (1987)).

The lateral motion model is described in terms of road lane curve tracking error in $\{xyz\}$. Considering expert drivers' behavior to observe the road at a look-ahead distance while driving, we describe the lateral motion model in terms of error at a look-ahead distance error (Fig. 2).

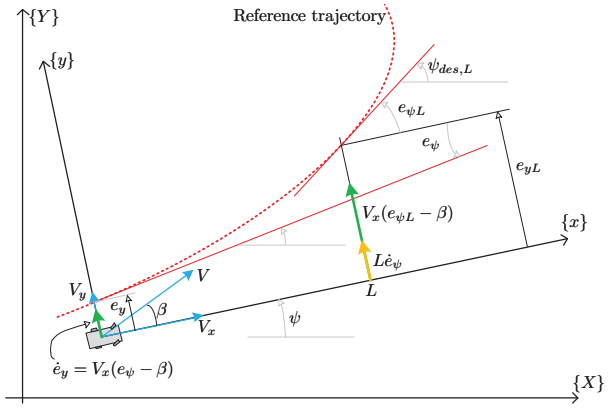

Fig. 2. Lateral position and velocity errors at the look-ahead distance point

Considering possible state measurements that may be conducted via the use of multiple sensors with different principles, the vehicle lateral motion is described in terms of the state vector $\mathbf{x} = \left[\mathbf{x}_v^T \ \mathbf{x}_m^T\right]^T$ with $\mathbf{x}_v = [e_{yL} \ \dot{e}_y \ e_\psi]^T$ and $\mathbf{x}_m = \left[\dot{\psi}\right]$, $\mathbf{u} = \delta$

$$\begin{aligned}\dot{\mathbf{x}} &= A\mathbf{x} + B\mathbf{u} + B_\varphi\varphi + B_\phi \sin\phi \\ &= \begin{bmatrix} A_v & A_{vm} \\ A_{mv} & A_m \end{bmatrix}\mathbf{x} + \begin{bmatrix} B_v \\ B_m \end{bmatrix}\mathbf{u} + \begin{bmatrix} B_{v\varphi} \\ 0 \end{bmatrix}\varphi + \begin{bmatrix} B_{v\phi} \\ 0 \end{bmatrix}\sin\phi \end{aligned} \tag{1}$$

where $\varphi = \left[\dot{\psi}_{des} \ \ e_{\psi L} - e_\psi\right]^T$,

$$A_v = \begin{bmatrix} 0 & 1 & 0 \\ 0 & a_{22} & a_{23} \\ 0 & 0 & 0 \end{bmatrix},\ A_m = [a_{44}],\ A_{vm} = \begin{bmatrix} -L \\ a'_{24} \\ -1 \end{bmatrix},$$

$$A_{mv} = \begin{bmatrix} 0 & a'_{42} & a_{43} \end{bmatrix},\ B_v = \begin{bmatrix} 0 \\ b'_{21} \\ 0 \end{bmatrix},\ B_m = [b_{41}],$$

$$B_{v\varphi} = \begin{bmatrix} L & V_x \\ V_x & 0 \\ 1 & 0 \end{bmatrix},\ B_{v\phi} = \begin{bmatrix} 0 \\ g \\ 0 \end{bmatrix}.$$

A detailed analytical derivation of the model is explained in (Lee et al. (submitted)).

For the ECU sampling period T_c, one can obtain the ZOH discrete-time equivalent quadruplet, to $(A, B, B_\varphi, B_\phi)$,

$$(\Phi, \Gamma, \Gamma_\varphi, \Gamma_\phi) = \left(\begin{bmatrix} \Phi_v & \Phi_{vm} \\ \Phi_{mv} & \Phi_m \end{bmatrix}, \begin{bmatrix} \Gamma_v \\ \Gamma_m \end{bmatrix}, \begin{bmatrix} \Gamma_{v\varphi} \\ 0 \end{bmatrix}, \begin{bmatrix} \Gamma_{v\phi} \\ 0 \end{bmatrix} \right).$$

3.2 Longitudinal Motion Model

Some part of longitudinal motion model are control softwares: The electronic stability control (ESC) control software and the cruise control software.

It is usual to design the ESC closed-loop system such that

$$G_{esc-clp} = \frac{\ddot{x}}{\ddot{x}^d} = \frac{1}{\tau s + 1}$$

where τ is typically 0.5 (see e.g. Rajamani (2006)). Moreover, the cruise controller G_{cc} is in a form of proportional-integral control. Then, it is immediate to find the closed-loop cruise control system transfer function

$$G_{cc-clp} = \frac{\dot{x}}{\dot{x}^d} = \frac{G_{esc-clp}G_{cc}}{s + G_{esc-clp}G_{cc}}$$

that describes high-level longitudinal vehicle motion. The vehicle's front fixed longitudinal position x in $\{xyz\}$ is simply an integration: $x/\dot{x} = 1/s$.

Remark 1. The longitudinal motion model $x/\dot{x} = 1/s$ is independent of the lateral motion model. The lateral motion model requires $\dot{x}$ from the longitudinal model.

3.3 Steering System Model

Some part of steering system are also control softwares: The 'AFDR control' and the 'steering control' in Fig. 3.

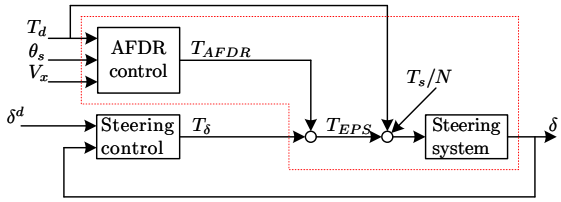

Fig. 3. Closed loop steering system with T_δ

The AFDR torque control can be expressed as $T_{AFDR} = T_A + T_F + T_D + T_R$, where T_A is the assistant torque (for driver's easy steering with steering torque $T_d + T_A$), T_F is the friction control (to compensate for mechanical friction increase due to T_d direction change), T_D is the damping control (to attain comfortable damped steering return with $T_s + T_D$), T_R is the return control (to attain neutral steering position $\theta_s = N\delta = 0$ when $T_d = 0$).

We describe the steering mechanism as a second order system. If the driver's torque $T_d = 0$, then the transfer function from T_δ to δ can be expressed as

$$G_{str} = \frac{\delta}{T_\delta} \approx \frac{1}{N(I_{swe}s^2 + C_{sw}s)}.$$

Once we design a steering servo controller G_{sc} (e.g. feedforward and PID control). Then, the closed-loop steering system transfer function $G_{sc-clp} = \delta/\delta^d$ can be readily computed. Further, it can be approximately described by

$$G_{sc-clp} = \frac{\delta}{\delta^d} \approx \frac{1}{\tau_s s + 1}$$

where τ_s is typically $0.1 \sim 0.2$ sec (our experimental observation).

4. VEHICLE LOCALIZATION

4.1 Multirate to Synchronous Sampling

Sensing in autonomous vehicle is inherently multirate. Let T_c be the control update period (that is equal to the sampling period of the vehicle's ECU, T_{ecu}), T_{cam} be the camera-vision processing system's update period, and T_{rad} be the radar update period.

Without loss of generality, we assume (can let) $T_{cam} = R_{mv}T_{ecu}$ and $T_{rad} = R_{mr}T_{ecu}$ for some integers $R_{mv} \geq 1$ and $R_{mr} \geq 1$. The vehicle's yaw rate $\dot{\psi}$ and longitudinal velocity V_x are measurable and available from the vehicle ECU at a sampling rate of $1/T_c$.

Let k, k_v and k_r denote the ECU, the camera, and the radar update indices, respectively. Then the synchronous time is represented by

$$t = kT_c = (k_v + i/R_{mv})T_{cam} = (k_r + j/R_{mr})T_{rad} \quad (2)$$

for $k, k_v, k_r \in \mathcal{Z} = \{0, 1, 2, \dots\}$ and $i \in \mathcal{Z}_v = \{0, 1, \dots, R_{mv} - 1\}$ and $j \in \mathcal{Z}_r = \{0, 1, \dots, R_{mr} - 1\}$. By (2), we mean that there exist some time index sets $(k), (k_v, i), (k_r, j)$ satisfying the time synchronous condition: e.g. $\mathbf{u}(k) = \mathbf{u}(k_v, i) = \mathbf{u}(k_r, j)$.

In the next subsections, utilizing the synchronous time, we are to perform vehicle localization and environment perception through multi sensor-data fusion at a fast rate of the vehicle's ECU using decentralized multirate state estimation using multirate sensing from the camera-vision sensor (lane curve and obstacle vehicles at T_{cam}), the radar sensor (obstacle vehicles detection at T_{rad}), and the inertia sensor (yaw rate, speed, etc.).

4.2 Multirate Decentralized State Estimation

Using the model (1), we design a multirate decentralized state estimator: A state estimator to estimate $\mathbf{x}_m$ is

$$\begin{cases} \bar{\mathbf{x}}_m(k+1) = \Phi_m \hat{\mathbf{x}}_m(k) + \Gamma_m \mathbf{u}(k) + \Phi_{mv} \hat{\mathbf{x}}_v(k_v, i) \\ \hat{\mathbf{x}}_m(k) = \bar{\mathbf{x}}_m(k) + L_{lm} \left(\mathbf{y}_m(k) - C_m \bar{\mathbf{x}}_m(k) \right) \end{cases} \quad (3a)$$

where L_{lm} is the state estimator gain that stabilizes $\Phi_m - \Phi_m L_{lm} C_m$. In this case, $\hat{\mathbf{x}}_v$ are all assumed to be available from the multirate state estimator for $\hat{\mathbf{x}}_v$ we are to design. In order to estimate the state $\mathbf{x}_v$, we are to use a multirate state estimator

$$\begin{cases} \bar{\mathbf{x}}_v(k_v, i+1) = \Phi_v \hat{\mathbf{x}}_v(k_v, i) + \Gamma_v \delta(k_v, i) + \Phi_{vm} \hat{\mathbf{x}}_m(k_v, i) \\ \qquad + \Gamma_{v\varphi} \dot{\psi}_{des}(k_v, i) + \Gamma_{v\phi} \sin\phi \\ \hat{\mathbf{x}}_v(k_v, i) = \bar{\mathbf{x}}_v(k_v, i) + L_{lv} \left(\mathbf{y}_v(k_v, 0) - C_v \bar{\mathbf{x}}_v(k_v, 0) \right) \end{cases} \quad (3b)$$

where L_{lv} is the state estimator gain to be determined.

Definition 1. A multirate state estimator is referred to as convergent if it is convergent at some sampling periods.

Admitting that the output measurement $y_v(\cdot)$ is available at each sampling instant $k_v T_{cam}$, we are to make the multirate state estimator (3b) convergent at the sampling period T_{cam}. Now, applying discrete-time lifting (see e.g. Kranc (1957); Meyer (1992)) leads to

$$\bar{\mathbf{x}}(k_v + 1, 0) = \left(\Phi_v^{R_{mv}} - \Phi_v^{R_{mv}} \tilde{L}_{lv} C_v \right) \bar{\mathbf{x}}(k_v, 0) + \sum_1^{R_{mv}} \Phi_v^n \mathbf{y}(k_v, 0).$$

with a definition of $\Phi_v^{R_{mv}} \tilde{L}_{lv} = \sum_1^{R_{mv}} \Phi_v^n L_{lv}$. Utilizing a gain $\tilde{L}_{lv}$ that stabilizes $\Phi_v^{R_{mv}} - \Phi_v^{R_{mv}} \tilde{L}_{lv} C_v$, we immediately compute

$$L_{lv} = \left(\sum_1^{R_{mv}} \Phi_v^n \right) \Phi_v^{R_{mv}} \tilde{L}_{lv}$$

that guarantees the convergence of the state estimator (3b) at each camera-vision processing update time.

Proposition 1. The decentralized multirate state estimators given in (3) are convergent, if their dynamics show convergence at some respective sampling periods.

Proof: Skipped due to space limitation. ■

4.3 Vehicle Localization

Vehicle localization on road is achieved by detecting road lane marks as a cloithoidal cubic polynomial. The vehicle motion model in terms of the road tracking error describes vehicle location on road: Vehicle localization.

The camera and vision processing system can provide a lane curve equation (see e.g., Dickmanns (2002))

$$f(x) = c_o + c_1 x + c_2 x^2 + c_3 x^3 \quad (4)$$

on the vehicle coordinate system, at a slow sampling rate of $1/T_{cam}$. Here, c_i's denote the lateral offset, heading angle error, curvature/2, curvature rate/6, respectively.

For robust road lane detection, we apply multirate multi-sensor data fusion using the multirate decentralized state estimation $C_v \hat{\mathbf{x}}_v$ in (3b) and the nonholonomic constraint on the clothoidal road model - slowly varying curvature $\kappa = 6c_3 V_x T_c + 2c_2$. By fusing these informations, we obtain an optimal road lane curve estimation in the case of intermittent faulty lane detection.

We first use $\bar{\mathbf{x}}_v(k_v, i)$ in (3b) to obtain a lane curve prediction at time (k_v, i): $\bar{c}_1 = \bar{e}_\psi(k_v, i)$, the heading angle error prediction, $\bar{c}_3 = c_3$, $\bar{c}_2 = \bar{\kappa}/2$ with a curvature prediction $\bar{\kappa} = 6\bar{c}_3 V_x T_c + 2c_2$, and $\bar{c}_0 = \bar{e}_{yL}(k_v, i) - \bar{c}_1 L - \bar{c}_2 L^2 - \bar{c}_3 L^3$. These coefficients can be used to build a lane curve prediction $\bar{f}(x)$.

It is our observation that the cubic polynomial lane curve $f(x)$ in (4) is very sensitive to the errors in the coefficients c_2 and c_3. By this we mean that erroneous detections of c_2 and c_3 by the camera-vision sensors may cause a fishtail curve to occur. In this regard, we need to evaluate reliability of a detection of lane curve using the Mahalanobis distance (see e.g. Thrun et al. (2006))

$$d_{M_f}^2(\bar{f}, f) = \left(\begin{bmatrix} \bar{c}_2 \\ \bar{c}_3 \end{bmatrix} - \begin{bmatrix} c_2 \\ c_3 \end{bmatrix} \right)^T R_f^{-1} \left(\begin{bmatrix} \bar{c}_2 \\ \bar{c}_3 \end{bmatrix} - \begin{bmatrix} c_2 \\ c_3 \end{bmatrix} \right) \quad (5)$$

where R_f denotes an error covariance matrix associated with the lane curvature and its rate. A lane curve detection is reliable and can thus be used, provided $d_{M_f}(\bar{f}, f)$ in (5) is less than a pre-specified threshold value. Otherwise, it is considered as a faulty lane curve detection that cannot be used.

Now, we can use $\hat{\mathbf{x}}_v(k_v, i)$ in (3b) to estimate the lane curve at time (k_v, i): $\hat{c}_1 = \hat{e}_\psi(k_v, i)$, the heading angle error estimation, $\hat{c}_3 = c_3$, $\hat{c}_2 = \hat{\kappa}/2$ with $\hat{\kappa} = 6\hat{c}_3 V_x T_c + 2c_2$, and $\hat{c}_0 = \hat{e}_{yL}(k_v, i) - \hat{c}_1 L - \hat{c}_2 L^2 - \hat{c}_3 L^3$. These coefficients can be used to build a lane curve estimation $\hat{f}(x)$.

5. ENVIRONMENT PERCEPTION

For autonomous driving, perception of environment (other vehicles around), in addition to on-road vehicle localization, must be used in producing a trajectory command. This section is dedicated to describing an innovative way to describe the results of environment perception and to determine a trajectory command utilizing it.

5.1 Control Block for Block-Wise Environment Perception

As far as we are concerned with safest driving, we are interested in determining risk-free environment rather than acceptable risk through a complex risk assessment to determine quantitative or qualitative value of risk related to lane keeping/changing.

In order to describe the results of environment perception in a block-wise manner, just determining risk-free or not, we propose a simple block-wise environment perception method referred to as *Control Block* (Fig. 4).

Assumption 1. Perception of environment in such a block-wise manner is available so as to determine the condition of each sub-block.

It should be noted that Assumption 1 just requires a simplest risk assessment. If an obstacle vehicle is already in, just entering, or expected to move into a sub-block (in the very short future), then the sub-block becomes red. Such a simple block-wise condition determination via environment perception is a very simple yet efficient risk assessment to determine admissibility of lane keeping/changing. In reality, as far as we are concerned about safest driving, quantitative or qualitative value of risk related to lane changing appears to be useless. By this we mean that we are simply interested in risk-free situation that leads to safest driving.

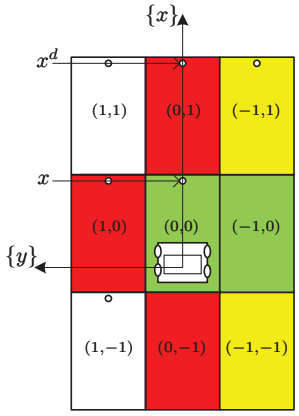

Fig. 4. Control block consists of 3×3 sub-blocks.

The control block, consists of 3×3 sub-blocks in $\{xyz\}$ is simply a block-wise description of the environment of the vehicle: The origin sub-block $\mathcal{B}(0,0)$ is taken by the vehicle, and the other sub-blocks are either vacant or (possibly) taken by surrounding vehicles. The (red-colored) occupied sub-blocks are taken by arounded vehicles. The (green-colored) admissible sub-blocks, among the vacant sub-blocks, are candidate targets the vehicle can move into. Some admissible sub-blocks (yellow-colored) can only be reached via detour sub-blocks.

Each sub-block has a width of a lane and a height of minimum safe platoon driving distance (described by the tip-to-tail headway position x). Let x in $\{xyz\}$ be a minimum tip-to-tail headway position representing a distance from the tip of the vehicle to the tail of leading block added to the longitudinal distance from the center of gravity to the tip (Fig. 4). With a longitudinal velocity of $\dot{x}$, the position x in $\{XYZ\}$ can be reached in a tip-to-tail headway time τ_x. The headway time is time taken by the vehicle to cover the headway distance. By keeping a constant headway position x, the velocity set point $\dot{x}^d$ can be kept constant. Increasng/descreasing the headway position x, with a fixed headway time τ_x, leads to a corresponding velocity set point adjustment.

5.2 Control Block Topology for Trajectory Command

In order to determine if a candidate target sub-block is admissible, we propose a method referred to as *Control Block Topology.*

Definition 2. In a case of moving from $\mathcal{B}(0,0)$ to a target sub-block $\mathcal{B}(i_t,j_t)$ (simply noted as $\mathcal{B}(0,0) \rightarrow \mathcal{B}(i_t,j_t)$), we define a *maneuvering sub-block set* $\mathcal{B}([0:i_t],[0:j_t])$ where $[0:i_t]$ ($[0:j_t]$) denotes ascending/descending integers to i_t (j_t) and $([0:i_t],[0:j_t])$ denotes a set of finite combinations of such ascending/descending integers. Further, in a case of moving $\mathcal{B}(0,0) \rightarrow \mathcal{B}(i_d,j_d) \rightarrow \mathcal{B}(i_t,j_t)$, we define a maneuvering sub-block set $\mathcal{B}([0:i_d],[0:j_d]) \cup \mathcal{B}([i_d:i_t],[j_d:j_t])$.

Remark 2. The maneuvering sub-block set $\mathcal{B}([0:i_t],[0:j_t])$ consists of finite combination of ascending/descending integers to $i_t(j_t)$.

Definition 3. In terms of the control block, a maneuvering in which the (edges and vertices of) origin sub-block $\mathcal{B}(0,0)$ never invade red sub-blocks in its maneuvering sub-block set is defined as *risk-free maneuvering.*

The following proposition addresses risk-free (never invading red sub-blocks) maneuvering (lane keeping/changing).

Proposition 2. A sub-block $\mathcal{B}(i_t,j_t)$ is admissible, if the set $\mathcal{B}([0:i_t],[0:j_t])$ includes no red sub-block. Further, if the set $\mathcal{B}([0:i_d],[0:j_d]) \cup \mathcal{B}([i_d:i_t],[j_d:j_t])$ includes no red sub-block, the sub-block $\mathcal{B}(i_t,j_t)$ becomes admissible via an admissible detour sub-block $\mathcal{B}(i_d,j_d)$.

Proof: Skipped due to space limitation. ■

Now, a target sub-block, $\mathcal{B}(i_t,j_t)$, for possible lane change is determined through the control block topology in Proposition 2. We then need to design a trajectory command for the controller we are to design.

For longitudinal maneuvering, a headway position x^d is given to move into $\mathcal{B}(0,j_t)$.

For lateral maneuvering, we introduce a *Virtual Lane Curve* (VLC) that passes through the center of the target sub-block $\mathcal{B}(i_t,j_t)$:

$$f^{vlc}(x) = f(x) + e_y^{vlc}$$

where e_y^{vlc} is the lane curve offset to the lane change direction from the lane curve at $\mathcal{B}(0,0)$.

Remark 3. The virtual lane curve at the target sub-block $\mathcal{B}(i_t,i_t)$ introduced for lane change from the origin sub-

block $\mathcal{B}(0,0)$ naturally becomes the real lane curve as the target lane is taken by the vehicle.

The trajectory command is given in terms of the state reference described by

$$\mathbf{x}^d = \begin{bmatrix} e_{yL}^{vlc} & \dot{e}_y^r & e_\psi^{vlc} & 0 \end{bmatrix}^T \tag{6}$$

where $\dot{e}_y^r$ denotes a desired decay rate of error associated with the VLC. By determining $\dot{e}_y^r$, one can adjust the lateral position error decay rate,

Assigning a target sub-block $\mathcal{B}(i_t, j_t)$ is equivalent to giving $(x^d, \mathbf{x}^d)$, a set of desired headway position and desired lateral pose error, that leads the vehicle to the target sub-block. By assigning a target/detour sub-block, a variety of autonomous driving scenarios can be realized: lane keeping with cruising, lane changing with cruising, lane changing with passing/being-passed-by other vehicles.

6. CONTROL DESIGN

The 'Trajectory Command' in Fig. 1 computes a reference set for vehicle maneuvering: a set of desired headway position and desired lateral pose error. Given a trajectory command $(x^d, \mathbf{x}^d)$, the 'Speed control' and the 'Lateral control' determine $(\dot{x}^d, \delta^d)$: The 'Speed control' generates a desired longitudinal velocity $\dot{x}^d$ that is to be applied to the cruise control closed-loop G_{cc-clp}, whilst the 'Lateral control' generates a desired steering angle δ^d that is to be applied to the steering control closed-loop G_{sc-clp}. The role of the 'Arbitration' in Fig. 1 includes determination of possible lateral control mode change.

6.1 Longitudinal Speed Control

The 'Speed control' in Fig. 1 generates a desired longitudinal velocity $\dot{x}^d$ that is to be applied to the cruise control closed-loop G_{cc-clp}.

For longitudinal speed control design, we propose a map to generate a velocity set point trajectory

$$\dot{x}^d = \dot{x} + \text{sat}\left(\frac{f_{vx}(x^d - x)}{\gamma_x T_c}\right)\gamma_x T_c \tag{7}$$

where $\gamma_x > 0$ is a design constant to limit the rate of change in longitudinal velocity such that $\left|\dot{x}^d - \dot{x}\right| < \gamma_x T_c$. A simple form of $f_{vx}(\cdot)$ is surely $(x^d - x)/\tau_x$. The velocity command $\dot{x}^d$ becomes an input to the cruise control closed-loop G_{cc-clp}. The desired longitudinal velocity $\dot{x}^d$ is expressed in terms of the desired and current headway positions.

6.2 Lateral Control

The 'Lateral control' in Fig. 1 generates a desired steering angle δ^d that is to be applied to the steering control closed-loop G_{sc-clp}.

For lateral control, we apply model predictive control (MPC) to generate a desired steering angle δ^d which becomes an input to the steering control closed-loop. The reference trajectory for MPC is determined as

$$\mathbf{r}(k+i) = e^{-\eta i} C \mathbf{x}^d(k), \quad i = 0, \ldots, N_p - 1 \tag{8}$$

where N_p is the prediction horizon and $\eta > 0$ is a design constant.

For real-time optimality of the lateral controller, we are to apply the multilevel approximate model prediction control for real-time optimality (see Lee and Chung (2013)). The predictive control scheme attains optimality the advantage of the predictive control while significantly saving computing time. Details are not given here due to space limitation. The interested readers are referred to the reference.

7. IMPLEMENTATION AND TESTS

The autonomous driving control system is implemented for in-vehicle tests on a test vehicle (Hyundai Tucson). The high-level commands $\dot{x}^d$, the velocity set point, and δ^d, the desired steering angle, generated from the 'speed control' and 'lateral control', respectively, in Fig. 1 are injected into the in-vehicle cruise controller as a velocity set point and the in-vehicle EPS system as a value aided function torque input, both thru the CAN communication. By this, the proposed autonomous driving control system is seamlessly integrated into the test vehicle with modification for implementation being minimized.

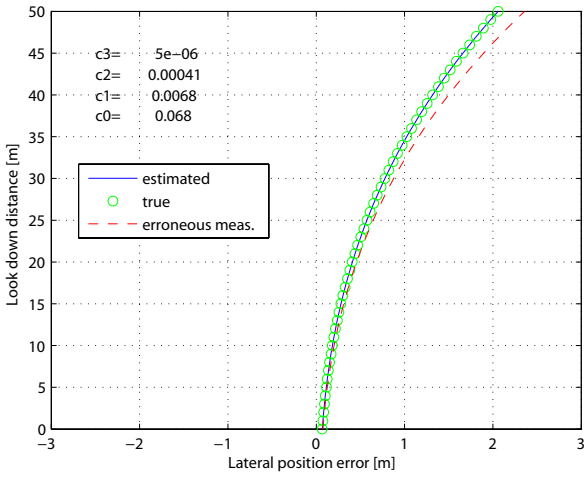

(a)

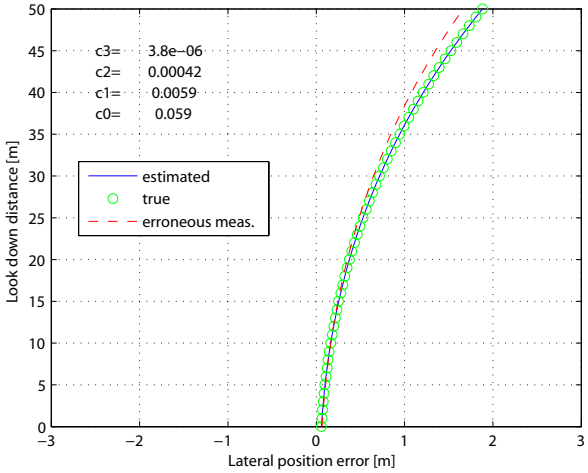

(b)

Fig. 5. Frame sequence in road lane curve estimation simulation: a fishtail curve by the camera-vision measurement error is corrected.

First, road lane curve estimation scheme is tested. A frame sequence in Fig. 5 demonstrates that the cubic polynomial

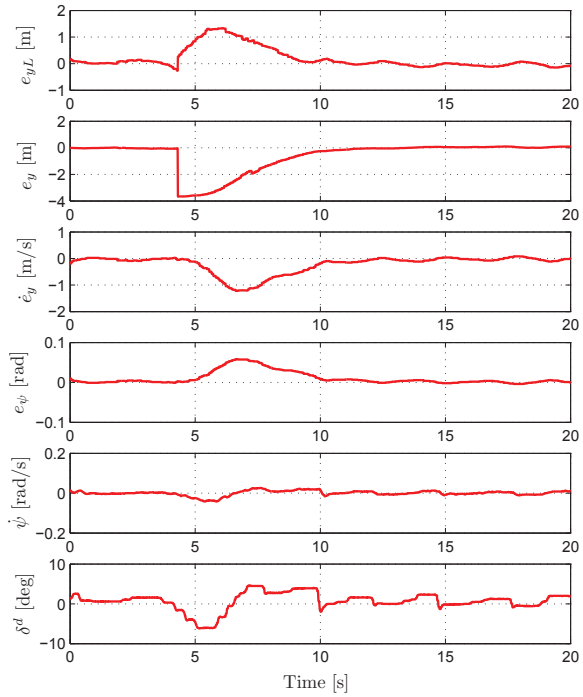

Fig. 6. Lane change experiment with a scenario of $\mathcal{B}(0,0) \rightarrow \mathcal{B}(-1,0)$

curve is very sensitive to the errors in the coefficients c_2 and c_3: even $\pm 10\%$ random errors cause such a problematic fish tail curve. We find that some intermittent camera-vision measurement errors/failures can be corrected by considering the vehicle motion and the clothoidal road model constraint.

We then conducted an autonomous lane changing experiment on a vehicle performance test track. As a safest lane change scenario, we tried a lane change at a vehicle speed of 30m/s on straight road lane with obstacle vehicles taking their sub-blocks $\mathcal{B}(0,-1)$, $\mathcal{B}(1,0)$, and $\mathcal{B}(0,1)$ in the control block (Fig. 4). By applying the control block topology, an admissible target sub-block $\mathcal{B}(-1,0)$ is determined for lane change. The predictive lateral controller with a reference trajectory (8) and the longitudinal speed controller in (7) are applied. The result of lane change experiment with a scenario of $\mathcal{B}(0,0) \rightarrow \mathcal{B}(-1,0)$ is shown in Fig. 6. The VLC is introduced at about 4.3s. Lane crossing occurs at about 7s. Lane change completes in 5.5s.

8. CONCLUSIONS

A systems approach has been proposed for autonomous driving control system development and implementation. The proposed autonomous driving control system framework dissected an automotive system into some subsystems with communications between them being considerred such that systematic control system designs can be accomplished. The proposed control block and control block topology used block-wise perception of environment and vehicle localization to produce a trajectory command via a virtual lane curve for longitudinal/lateral vehicle control. As shown through an application, the proposed autonomous driving control system and its design methods allow a systematic autonomous driving control design to be accomplished in a systems approach, well developed variety of control and estimation theories can be easily applied with readiness for seamless implementation.

REFERENCES

Dickmanns, E. (2002). The development of machine vision for road vehicles in the last decade. In *IEEE Intelligent Vehicles Symposium*, volume 1. IEEE.

Falcone, P., Borrelli, F., Asgari, J., Tseng, H., and Hrovat, D. (2007). Predictive active steering control for autonomous vehicle systems. *IEEE Trans. Control Syst. Technol.*, 15(3), 566–580.

Guldner, J., Sienel, W., Tan, H., Ackermann, J., Patwardhan, S., and Bunte, T. (1999). Robust automatic steering control for look-down reference systems with front and rear sensors. *IEEE Trans. Control Syst. Technol.*, 7(1), 2–11.

Hatipoglu, C., Özgüner, Ü., and Redmill, K. (2003). Automated lane change controller design. *IEEE Trans. Intelligent Transportation Systems*, 4(1), 13–22.

Hedrick, J., McMahon, D., Narendran, V., and Swaroop, D. (1991). Longitudinal vehicle controller design for IVHS systems. In *Amer. Contr. Conf.*, 3107–3112. IEEE.

Ioannou, P., Xu, Z., Eckert, S., Clemons, D., and Sieja, T. (1993). Intelligent cruise control: theory and experiment. In *Conf. Decision Contr.*, 1885–1890. IEEE.

Kranc, G.M. (1957). Input-output analysis of multirate feedback systems. *IRE Trans. Automatic Control*, 21–28.

Lee, S.H. and Chung, C.C. (2013). Multilevel approximate model predictive control and its application to autonomous vehicle active steering. In *Conf. Decision Contr.*, 5746–5751.

Lee, S.H., Son, Y., and Chung, C. (submitted). Autonomous driving vehicle control: A systems approach to development and implementation. *IEEE Trans. Control Syst. Technol.*

Li, S., Li, K., Rajamani, R., and Wang, J. (2010). Model predictive multi-objective vehicular adaptive cruise control. *IEEE Trans. Control Syst. Technol.*, (99), 1–11.

Meyer, D.G. (1992). Cost translation and a lifting approach to the multirate LQG problem. *IEEE Trans. Autom. Control*, 37, 1411–1415.

Möbus, R., Baotic, M., and Morari, M. (2003). Multi-object adaptive cruise control. *Hybrid Systems: Computation and Control*, 359–374.

Pacejka, H.B., Bakker, E., and Nyborg, L. (1987). Tyre modelling for use in vehicle dynamics studies. *SAE paper*.

Pham, H., Hedrick, K., and Tomizuka, M. (1994). Combined lateral and longitudinal control of vehicles for IVHS. In *Amer. Contr. Conf.*, volume 2, 1205–1206. IEEE, Baltimore, MD, USA.

Rajamani, R. (2006). *Vehicle dynamics and control*. Springer.

Rajamani, R., Tan, H., Law, B., and Zhang, W. (2000). Demonstration of integrated longitudinal and lateral control for the operation of automated vehicles in platoons. *IEEE Trans. Control Syst. Technol.*, 8(4), 695–708.

Thrun, S., Burgard, W., and Fox, D. (2006). *Probabilistic Robotics*. The MIT Press.